NUKLEONIKA 2006;51(Supplement 1):S27–S33

PROCEEDINGS

Synthesis of nanostructured tetragonal ZrO_2 of enhanced thermal stability

Andrzej Adamski,
Paweł Jakubus,
Zbigniew Sojka

Abstract Hydrous zirconia particles of nanometric dimensions were synthesized via forced hydrolysis of zirconyl chloride. Prolonged aging at 100°C in the mother liquor and subsequent calcination produced a single-phase tetragonal ZrO_2 of enhanced thermal stability with the narrow size and pore distributions. The influence of the preparation conditions on the phase composition of the resultant zirconium dioxide was examined using structural (XRD, SEM/TEM) and spectroscopic (Raman) methods, supported by thermal analysis (DTA/TG, DSC) and N_2-porosimetry. The nature of the parent salt, pH of the solution, the temperature of precipitation and aging, were found to be the key parameters of the successful synthesis. The sequence of mechanistic steps invoked to account for the formation of t-ZrO_2 was rationalized using the concepts of zirconium aquatic chemistry.

Key words nanostructured tetragonal ZrO_2 • preparation • aging • crystallization • sintering • aquatic chemistry

A. Adamski
Faculty of Chemistry,
Jagiellonian University,
3 Ingardena Str., 30-060 Kraków, Poland,
Tel.: +48 12 663 2224, Fax: +48 12 634 0515,
E-mail: adamski@chemia.uj.edu.pl

P. Jakubus
Institute of Chemistry and Environment Protection,
Szczecin Technical University,
42 Piastów Ave., 71-065 Szczecin, Poland

Z. Sojka
Faculty of Chemistry, Jagiellonian University,
3 Ingardena Str., 30-060 Kraków, Poland
and Regional Laboratory of Physicochemical
Analyses and Structural Research,
3 Ingardena Str., 30-060 Kraków, Poland

Received: 14 November 2005
Accepted: 16 February 2006

Introduction

Zirconium dioxide, owing to its mechanical, thermal and chemical properties is an attractive ceramic material of various applications, which has received a great deal of research interest [14, 21, 29]. Upon chemical and textural valorization, it is also frequently used as catalyst or catalyst support [12, 22, 28]. In the latter context, zirconia may serve as a paramount example of strong dependence of the surface properties (and related catalytic activity) on the bulk structure, controlled by the nature of its polymorphic form [19]. Preparation of ZrO_2 by conventional precipitation from aqueous solutions of the zirconyl salts leads usually to a mixture of the stable monoclinic m-ZrO_2 and metastable tetragonal t-ZrO_2 forms. However, the phase transformation between the monoclinic and the tetragonal polymorph, due to the large volume change (ca. 47%), prevents the unique properties of bare zirconia to be used in practice directly. Such disruptive phase transition can be suppressed by stabilization of t-ZrO_2 either via appropriate cationic doping [14] or by tailoring the size of particles below the critical value of $r_0 \sim 30$ nm, which gives rise to so-called TZP (tetragonal zirconia polycrystals) ceramic [13]. The resultant nanostructured t-ZrO_2 exhibits distinctly different properties in comparison to the coarse-grained m-ZrO_2 and t-ZrO_2. Therefore, the use of appropriate preparation procedures, leading to desired form of the zirconium oxide, is required for specific applications [7, 26].

A common route for the preparation of zirconia consists in precipitation of hydrous gel with ammonia from zirconyl salt solutions and subsequent calcination of the amorphous precipitate. The crystallization, which usually occurs in the temperature range of 370–400°C, as well as the phase composition of the resultant oxide, are severely affected by the processing parameters such as pH of the solution, concentration of the zirconyl salt, the nature of counter anions, precipitation temperature and aging conditions [12, 21]. Alien chemical species (mineralizers) [11] present in the solution, in which the precipitate is aged, can also affect the crystallization behavior, in favor of the tetragonal polymorph [17]. Usually, the metastable t-ZrO_2 tends to disappear at temperatures above 600°C, which are often too low for many practical applications. Therefore, it is essentially important to ascertain a sufficient stability of the resultant t-ZrO_2 by an appropriate chemical treatment, in the possibly largest temperature window.

The crystalline structure of the three ZrO_2 polymorphs: tetragonal ($P4_2/nmc$), monoclinic ($P2_1/c$) and cubic ($Fm3m$) is well established [27]. In contrast, the chemical nature of hydrous precursors, as well as complex transformations occurring in aqueous solution during precipitation, hydrothermal treatment and subsequent calcination of the samples, are still far from being definitely understood. These problems, having their source in aquatic chemistry of zirconyl solutions, are of great importance for optimization of the structural modifications of the final zirconia preparations. The aquatic chemistry of zirconium is featured by its tendency to form inorganic polymers via oxolation and olation processes [9]. The resultant oligomeric species, depending on their particular molecular structure and the extent of a framework development, will give rise to different zirconia polymorphs [4]. Upon hydrothermal treatment, amorphous zirconia exhibits a relatively well ordered, molecular framework compatible with the tetragonal ZrO_2, which may serve as a template for crystallization of the metastable t-ZrO_2 as a single phase [25].

In the present paper, the influence of the preparation method and aging of the precipitate on the nucleation, crystal growth, phase composition and surface properties of the resultant zirconium oxide was investigated using several techniques (XRD, TEM/SEM, Raman, DTA/TG, DSC and N_2-porosimetry. The aim was to establish optimal synthesis conditions for obtaining nanostructured t-ZrO_2 of enhanced thermal stability.

Experimental

Hydrous zirconia samples were obtained by precipitation from aqueous solutions of $ZrOCl_2 \cdot 8H_2O$ and $ZrO(NO_3)_2 \cdot H_2O$ (Aldrich 99.99%) with a 25% aqueous solution of ammonia, at various concentrations (from 0.006 to 0.6 M) and temperatures (ranging from room temperature to 100°C). To examine the influence of aging on the phase composition of the resultant oxide, the samples were divided into two parts. The first part was separated from the mother liquor and dried without previous digestion (aging), whereas the second one was aged at various temperatures for 48 h under reflux, while maintaining the pH at ~ 9, by periodical addition of $NH_{3(aq)}$. The resultant zirconia gel was washed with dilute NH_4NO_3 solution until negative test for Cl^- ions, then dried at 100°C for 24 h, and finally calcined in air at 600°C for 6 h.

X-ray diffraction patterns of the dried and calcined samples were recorded on a DRON-3 diffractometer (Bourevestnik, Russia) equipped with an iron filter, using CuK_α and CoK_α radiations. The phase composition of the samples was calculated from the following relationships:

$$X_t = I_t(111) / [I_t(111) + I_m(111) + I_m(11\bar{1})] \qquad (1)$$
$$X_m = 1 - X_t$$

where X_t and X_m indicate the fraction of the tetragonal and the monoclinic forms, respectively, whereas I_t and I_m are the intensities of their diagnostic peaks [22].

The SEM microstructural analysis was performed using a JEOL JSM-1600 microscope equipped with an ISIS 300 (Oxford) microanalyzer. High resolution transmission electron microscopy (HR-TEM) was carried out using a JEM-100CX II UHR instrument (JEOL) operating at 100 kV. The specimens were prepared by deposition of the samples, which were ultrasonically dispersed in ethanol, on a holey carbon film supported on a copper grid. The size of the particles (an average diameter of 40–60 particles sampled at random) was assessed from the corresponding micrographs.

Raman spectra were collected on an FTS 6000 spectrometer equipped with a BIORAD accessory. The samples were excited with 1064 nm line of a diode-pumped Nd:YAG laser (Spectra Physics Model T108S) and the scattered radiation was collected at 180° with 4 cm^{-1} resolution.

Differential thermal and gravimetric analysis (DTA/TG) and differential scanning calorimetric measurements (DSC) were carried out in the nitrogen or helium flow using a SDT 2960 and a DSC 2010 (TA Instruments) apparatus, respectively. The heating rate was 10°C/min.

The specific surface area was determined according to the BET method [3]. The N_2-sorption isotherms were measured at the liquid nitrogen temperature, using a Micromeretics ASAP 2010 system. Prior to the measurements, the samples were outgassed at 623°C for 10 h. The pore volume and the pore size distribution were calculated from adsorption isotherms, basing on the Barrett-Halenda-Joyner (BHJ) [2] and Horvath-Kawazoe (HK) [16] formalisms.

Results

Influence of precipitation conditions on the structure of ZrO_2

To evaluate the importance of precipitation parameters on the phase composition of the final product in a systematic manner, a preparation protocol shown in Fig. 1 was applied. The influence of five different preparation variables such as the nature and concentration of the starting precursor, the pH of parent solution, the presence of additives as well as the temperature of precipitation and aging on the phase composition of ZrO_2 was examined.

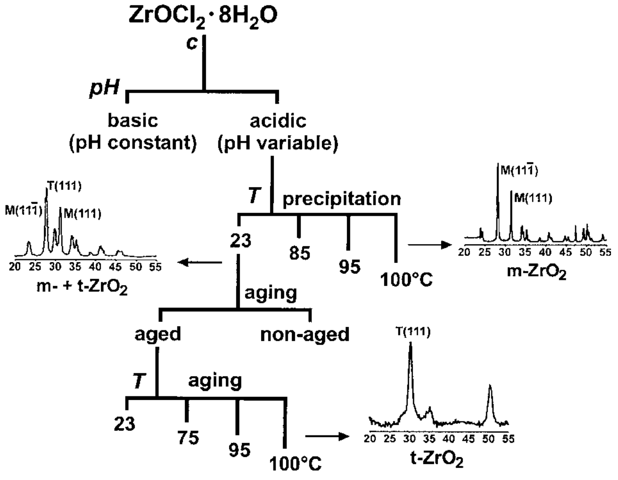

Fig. 1. The protocol for synthesis of zirconium dioxide of the controlled phase composition and the corresponding XRD patterns (CuK_α).

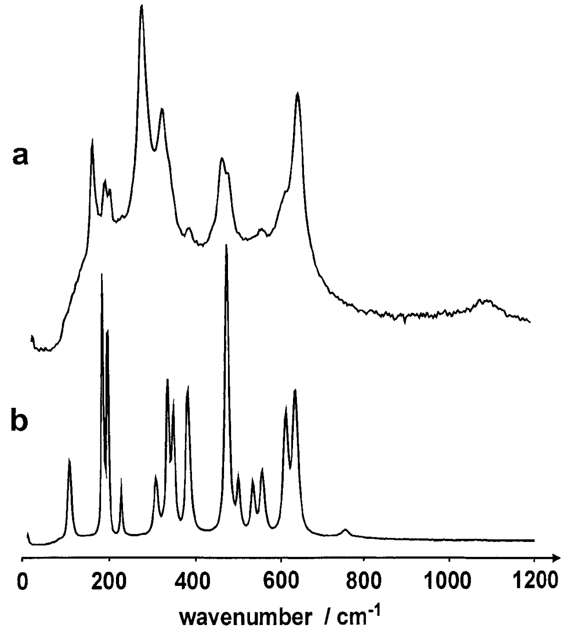

Fig. 2. Raman spectra of (a) t-ZrO_2 (aged sample calcined at 600°C for 6 h), and (b) m-ZrO_2 (non-aged sample, calcined at 1000°C for 6 h).

Using Eq. (1), the content of the tetragonal polymorph can be determined easily, from the intensity of the corresponding X-ray diffraction lines in the diagnostic 2θ region between 25 and 33° (CuK_α) or 31 and 38° (CoK_α), where the (111) reflection of the tetragonal phase and the $(11\bar{1})$ and (111) reflections of the monoclinic phase appear [22]. In addition to XRD measurements, the phase composition of the samples was verified by Raman spectroscopy, which is much more sensitive to small differences in the position of oxygen ions, characteristic of different zirconia polymorphs. This latter property allows for facile distinction between the cubic and tetragonal zirconia, which, by using XRD alone, is much more demanding. The factor group theoretical analysis predicts 18 ($9A_g + 9B_g$) Raman active modes for the monoclinic ZrO_2 form, 6 ($A_{1g} + 2B_{1g} + 3E_g$) for the tetragonal ZrO_2 and only one F_{2g} mode for the cubic polymorph [15, 24]. These differences are clearly reflected in the Raman spectra (Fig. 2), where the small number of bands observed for the aged sample allows to identify the t-ZrO_2 phase quite readily (Fig. 2a), whereas for the non-aged sample, subjected to subsequent calcination at 1000°C, the each structure indicates that the sample consists of the m-ZrO_2 phase (Fig. 2b).

The t-ZrO_2 fraction in the samples changed from 20.5% for the non-aged ZrO_2, prepared by stepwise addition of ammonia to the $ZrOCl_2$ solution to 100% for the aged sample obtained by the same procedure (Fig. 1). During the synthesis, the pH changed from the initial value characteristic of the 0.6 M solution of the zirconyl chloride ($pH = 1.2$) to the final value of the ammonia buffer ($pH = 9.3$). Such *modus operandi* will be referred to hereafter as acidic method. In the case of basic method, where the sequence of mixing of both components is reversed (the zirconyl chloride solution is added directly to the concentrated ammonia solution at the constant pH kept at 9.3), the content of t-ZrO_2 did not exceed 55%, for both the aged and non-aged samples [17].

The temperature of precipitation and the thermal conditions of subsequent aging were also found to be important factors governing the phase composition of the final ZrO_2 (Fig. 3). Only for the samples precipitated at room temperature a single phase t-ZrO_2 was obtained upon aging (Fig. 3d). When the precipitation temperature was increased to 85°C (not reported here), the content of t-ZrO_2 dropped strongly down to just few percents, and at 100°C almost pure m-ZrO_2 was produced (Fig. 3b).

As it can be inferred from the XRD pattern (Fig. 3c), digestion in ambient conditions caused a rather small improvement of the t-ZrO_2/m-ZrO_2 ratio, in comparison to that of non-aged preparation (Fig. 3a). However, it rapidly increased from ~ 20% of t-ZrO_2 at 75–95°C to 100% of t-ZrO_2 when the temperature of aging was enhanced to 100°C (Fig. 3d). Thus, undoubtedly the acidic method of zirconia preparation, followed by prolonged aging of the precipitate at 100°C appeared to be the best way of obtaining a single phase t-ZrO_2, upon calcination of the $ZrO_2 \cdot xH_2O$ gel at 600°C for 6 h.

From the viewpoint of the t-ZrO_2 content in the final oxide, the nature of the precursor plays also an important role. This can be inferred from our studies where both $ZrOCl_2$ and $ZrO(NO_3)_2$ salts were used as precursors. Chlorides appear to be superior as a parent compound for preparation of the tetragonal nanozirconia in comparison to nitrates used in the same concentration (0.6 M) and subjected to the same acidic preparation method. The content of t-ZrO_2 in the latter case was not higher than 60%. It is worth noting here that the precursor effect cannot be leveled off by subsequent aging. The extent of metastabilization of t-ZrO_2, as gauged by the phase composition of the calcined zirconia sample, was remarkably lower for nitrates.

In comparison to the pronounced influence of the precursor nature and the pH of the parent solution, the concentration of the precursor seems to be less important. Despite that the content of t-ZrO_2 varied

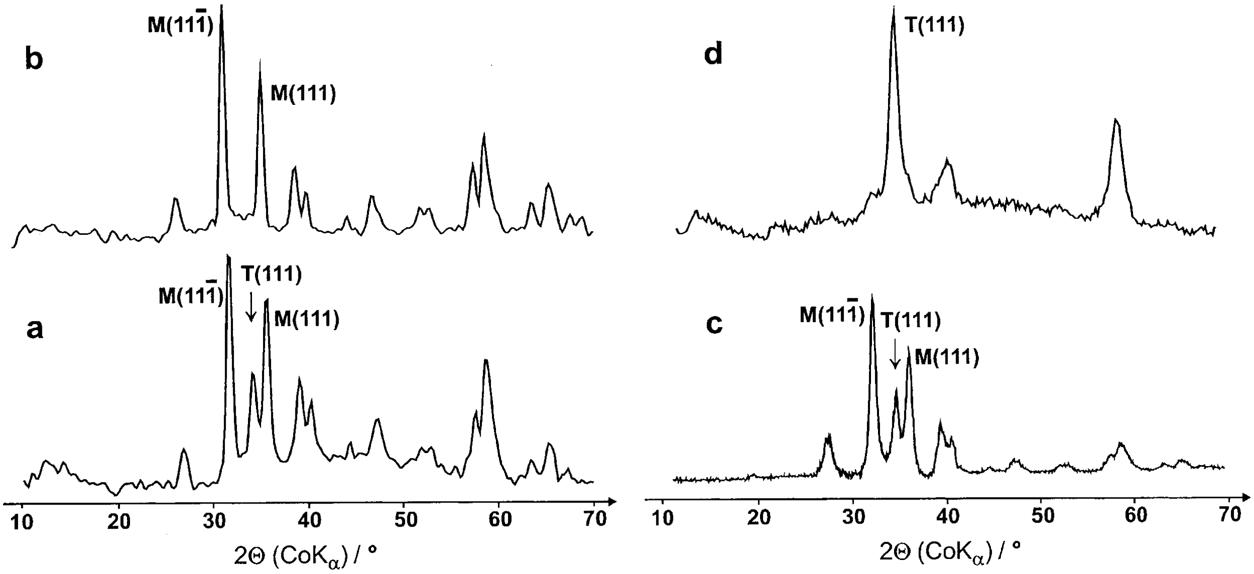

Fig. 3. XRD patterns obtained after calcination of hydrous zirconia at 600°C for 6 h. The non-aged sample prepared (a) by precipitation at room temperature, (b) precipitated at 100°C, (c) the sample aged and precipited at room temperature, (d) aged at 100°C for 48 h.

from 20.0 to 63.2% for non-aged samples prepared from $ZrOCl_2$ solutions of the concentration ranging from 0.006 to 0.6 M, all these specimens became fully tetragonal after the aging. For the raw samples, higher concentrations of the $ZrOCl_2$ solution favored crystallization of the t-ZrO_2 polymorph. This can readily be accounted for within the tenets of the classical nucleation and growth mechanism [18]. The size of particles that were formed at a given precursor concentration is linked to the relative nucleation and growth rates. With the increasing concentration, the nucleation, being much more sensitive to this parameter than the growth, tends to dominate. As a result, the rate of formation of new nuclei dominates their growth, decreasing the size of the final particles. This obviously favors the tetragonal polymorph that is stabilized by enhanced dispersion, owing to smaller surface energy in comparison to m-ZrO_2 [13]. The average size of the particles depends on the number of nuclei and the amount of the precursor available during the synthesis, but the particle size distribution is related to the specific mechanism of the nuclei growth.

Influence of aging on the progress of crystallization and particle growth

The crystallization progress of the zirconia gel was followed by the VT-XRD technique. The aged sample remained amorphous until 450°C and its transformation into t-ZrO_2 was accomplished at 530°C. As we learned from the results of a detailed thermal analysis [17], the process of ZrO_2 formation is quite complex and involves several mutually related steps such as dehydration of hydrous zirconia, nucleation of ZrO_2 proto-structures and coalescence of primary particles [20]. In the DTA/TG curves, an endothermic mass loss of 36% for the non-aged samples, associated with dewatering, was considerably higher for the aged samples (45%). The loosely bound water was released at temperatures below 170°C, whereas the reticular water persisted till 450°C upon heating. Such results show that digestion led to incorporation of considerable amounts of water into the framework of the gel. Another noteworthy feature of the prolonged digestion was an increase in the activation energy for dehydration (from 36.6 to 51.8 kJ/mol) and coalescence (from 233 to 300 kJ/mol), which was accompanied by disappearance of a glow phenomenon, observed at 400°C for the non-aged samples. Thus, upon aging the enhanced stabilization of the particles can be associated not only with the phase transformation to the tetragonal structure, but also with considerable lowering of the surface energy of the resultant t-ZrO_2, owing to preferential erosion of high energy facets. All those points are discussed below in more detail.

Aging in the mother liquor led to both: enhancement of the t-ZrO_2 content in the final solid (Fig. 3), and to a more uniform particle size distribution. The latter was revealed by analysis of the TEM micrographs, which for the non-aged samples exhibited a broad distribution of the particles size, ranging from 20–70 nm. In the case of aged samples a narrow size distribution with a maximum at 15 nm, distinctly below the critical value of 30–40 nm, was observed.

The aging was also responsible for enhancement of the specific surface area, accompanied by the development of micro- and of mesoporosity. The BET surface area measured for ZrO_2 samples calcined at 600°C for 6 h was equal to 23 m^2/g for the non-aged sample and to 77 m^2/g for the sample aged at 100°C for 24 h [17]. An over three-fold increase in the specific surface area is fully consistent with the diminishing particle size, due to the partial dissolution of zirconia in highly basic medium, and an increase of the pore volume from V_p = 0.046 to 0.214 cm^3/g. The latter phenomenon is essentially connected with the development of a bimodal porosity, exhibiting a narrow maximum at 15 nm and a broad one at ca. 100 nm. In the case of the

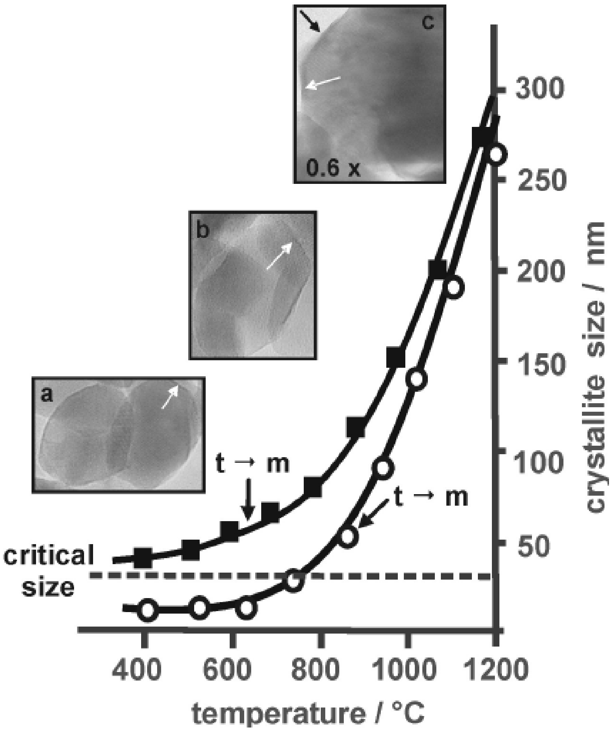

Fig. 4. Development of the particle size upon sintering of the non-aged (■) and the aged (○) zirconia samples, with the associated TEM micrographs corresponding to (a) 475, (b) 600, (c) 1000°C.

non-aged samples, the mesoporosity was distinctly suppressed, and the pore diameter shifted toward lower values (11 nm), but no microporosity was observed. In contrast, for the aged samples a regular monomodal distribution of micropores with a maximum at 0.51 nm appeared after the digestion [17].

As already mentioned, for practical applications thermal stability of the t-ZrO_2 polymorph and retention of its textural characteristics are of great importance. Zirconia prepared without the prolonged aging at 100°C, being a mixture of the t-ZrO_2 and m-ZrO_2 polymorphs, sinter more readily than the aged sample of more stable structure. As it can be inferred from the VT-XRD and TEM experiments (Fig. 4), calcination of the non-aged ZrO_2 caused a pronounced increase of the particle size due to the rapid coalescence of the primary particles and their sintering. Parallel TEM images revealed that the average diameter of the non-aged crystallites calcined at 475°C grew from 23 nm up to 33 nm at 600°C (Figs. 4a and 4b). After calcination at the temperature of 1000°C, the size of crystallites reached a value of 69 nm (Fig. 4c). On the contrary, the average diameter of the ZrO_2 crystallites in the aged samples was quite stable in the temperature range 400–800°C, and did not exceed the critical value of 30 nm. Fast sintering was observed only just after the phase transition to monoclinic form, which started at 850–950°C. This means that the applied preparation method combined with aging allowed for obtaining a tetragonal ZrO_2 of thermal stability enhanced by 250°C, in comparison to the non-aged samples. Specific surface area and pore structure were also preserved in this temperature range.

Discussion

Aquatic chemistry of zirconium(IV) salts

The mechanism of formation of hydrous zirconia from zirconyl precursors is strongly connected with its aquatic chemistry. When $ZrOCl_2 \cdot 8H_2O$ is dissolved in water, cyclic tetramer complexes $[Zr(OH)_2 \cdot 4H_2O]_4^{8+}$ are formed as dominant entities [10]. Gradual addition of ammonia to the solution resulted in dramatic changes in pH, forcing the hydrolysis of zirconium cations. In such conditions, the tetramers release protons from the terminal water to form $[Zr(OH)_{2+n} \cdot (4-n)H_2O]_4^{(8-4n)+}$ species, according to the equation [8]:

$$(2) \qquad [Zr(OH)_2 \cdot 4H_2O]_4^{8+} \leftrightarrow \\ \leftrightarrow [Zr(OH)_{2+n} \cdot (4-n)H_2O]_4^{(8-4n)+} + 4nH^+$$

Subsequent polycondensation takes place by olation ($Zr\text{-}OH + H_2O\text{-}Zr \rightarrow Zr\text{-}OH\text{-}Zr + H_2O$) and oxolation ($Zr\text{-}OH + HO\text{-}Zr \rightarrow Zr\text{-}O\text{-}Zr + H_2O$) processes leading to the formation of hydroxyl- and oxo-bridges between tetramer units, respectively. The empirical criterion for condensation to occur states that the partial charge on OH groups has to be negative, $\delta(OH) < 0$, since the hydroxyl groups should exhibit a nucleophilic character, and that on the metal ions distinctly positive ($\delta(Zr) > 0.3$), for the metal center has to be sufficiently electrophilic [18]. Such conditions are fulfilled for the zirconium tetramer species. Formation of the resultant solid precipitate involves three principal mechanistic steps: (i) formation of a zero-charge precursor oligomer, (ii) nucleation of incipient particles by condensation of the precursor oligomers, (iii) particle growth.

The shift in equilibrium of the hydrolysis (Eq. (2)), which changes the number of the hydroxyl ligands available for bridging, can easily be controlled by pH of the solution. This influences the specific course of the polycondensation process and subsequent water elimination during successive drying of the precipitate. Rapid addition of ammonia (basic method) increases the number of the terminal hydroxyls in the tetramer units in a random fashion, so that polycondensation occurs rapidly and in many directions at once. There is no time to form an ordered array of tetramers and the product of such a preparation procedure is an amorphous gel (Fig. 5a), which upon crystallization gives rise to m-ZrO_2 or a mixture of m-ZrO_2 and t-ZrO_2 (Fig. 1). In contrast, hydrolytic polycondensation induced by the acidic method is a slow process leading to progressive reticulation of the tetrameric units to form two-dimensional sheets of $[ZrO_x(OH)_{4-2x} \cdot yH_2O]_n$ as discussed elsewhere [8, 9]. The growth of the sheets leads to the formation of well structured primary particles of hydrous zirconia gel (Fig. 5b), when the critical size of the nucleation is reached. On heating, they act as a template, directing the crystallization toward the formation of tetragonal phase. The transformation of an amorphous gel to a metastable tetragonal zirconia is attributed to the loss of the hydration water, and the water produced during the olation process.

The influence of the parent zirconium salt on the phase composition of the final zirconium dioxide has

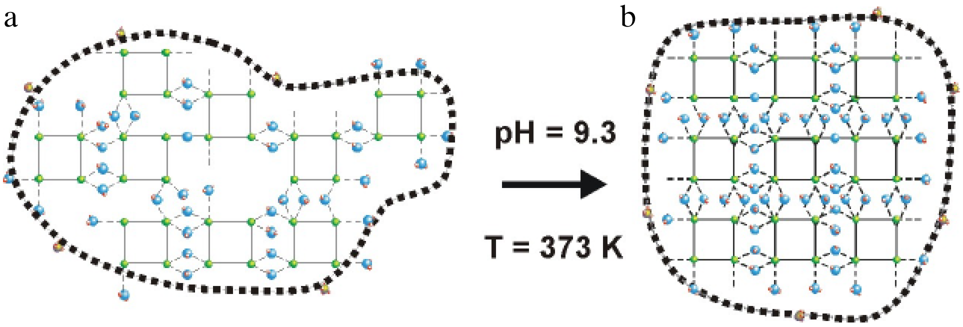

Fig. 5. Schematic picture of the molecular network of hydrous gel of zirconia for (a) the non-aged and (b) the aged sample (after Ref. [8]). In this figure: • stands for the Zr^{4+} ions, and ● – for the H_2O or OH groups.

already been noted [1, 23]. The reason for this phenomenon is the presence of polymeric zirconium species, which persist in solution. The degree of polycondensation can vary with the composition of the precursor, especially in the case of oxynitrates [1]. The properties of the precipitated gel are also influenced by the nature of the anions present in the solution, because the equilibria of complexation and hydrolysis control the rate of polymerization of zirconium species. The counter anions incorporated during the hydrolysis and condensation, according to the equation:

$$(3)\qquad [Zr(OH)_2 \cdot 4H_2O]_4^{8+} + 4nCl^- \leftrightarrow \\ \leftrightarrow [Zr(OH)_{2-n}Cl_n \cdot (4-n)H_2O]_4^{(8-4n)+}$$

may remain within the structure of hydrous zirconia. Complexation of the chloride ions takes place between pHs 5–11, whereas the nitrates do not form complexes with zirconium, apart from highly acidic conditions [18]. By replacing the bridging hydroxyl groups, such foreign anions may significantly modify the formation of the gel network as they reduce the number of OH^- groups that could be involved in the olation and oxolation processes. As a result, the anion should not be too strongly complexing, because it remains then in the precipitate. It should be neither too weakly complexing (nitrates), because just after dissolution of such precursor in water, rapid uncontrollable hydrolysis of Zr(IV) takes place, leading to highly disordered structure, which crystallizes into the mixture of t-ZrO_2 and m-ZrO_2. Comparison of the results, obtained using nitrite and chloride precursor salts, indicate that chloride ions seem to exhibit the optimal complexing properties for obtaining a tetragonal phase in aqueous conditions.

Role of aging

Aging in the suspension may lead to various modifications of the resultant precipitate such as change in particle size and morphology or even cause the crystallization of amorphous particles [18]. Usually, it is manifested in a shift of the size distribution due to the growth of large particles at the expense of small ones (Ostwald ripening). However, in the case of zirconia, this process may be complicated because of the large difference in the surface energy between t-ZrO_2 (γ_t = 0.77 J/m^2) and m-ZrO_2 (γ_m = 1.13 J/m^2) polymorphs [5]. In particular circumstances, this may lead to the appearance of a thermodynamic incentive favoring an opposite process.

The surface energy of zirconium oxide is considerably anisotropic with the (111) planes being the most stable and the (100), (110) planes the least stable for t-ZrO_2, whereas for m-ZrO_2 the most stable are the $(11\bar{1})$ planes and the (111) planes are distinctly less stable [5, 6]. Thus, an additional stabilization of the nanostructured t-ZrO_2 can be achieved by preferential erosion of the high energy facets, upon prolonged digestion of the precipitate. Following the Gibbs-Kelvin equation:

$$(4)\qquad S_r/S_\infty = \exp(2\gamma V/rkT)$$

where S_r and S_∞ indicate the solubility of a particle with radius r and that of a flat surface, respectively, we may expect that facets of different surface energy γ will exhibit different solubilities. Digestion in a strongly basic medium by preferential erosion of high energy planes should, therefore, lead to restructuring of the morphology of zirconia particles, as it is shown schematically in Fig. 5. This is consistent with the TEM pictures and with observed loss of the glow phenomenon in the course of the coalescence in DSC measurements. In addition, a sequence of crystallization-dissolution processes, occurring during aging, gives rise to reticulation of the hydrous zirconia precipitate via deoxolation, constituting an apposite proto-structure for direct crystallization into the t-ZrO_2 polymorph. Another beneficial effect of aging is the stiffening of the hydrated gel, which inhibits the extent of shrinkage that takes place during drying and subsequent calcination.

Conclusions

Successful synthesis of metastable tetragonal zirconium oxide of enhanced thermal stability by forced hydrolysis of aqueous $ZrOCl_2$ solutions using the acidic method was described. The role of the principal preparation variables controlling the phase composition and thermal stability, such as pH, concentration and temperature of the solution, the nature of parent zirconium salt as well as aging of the precipitate was evaluated. It was shown that extended digestion of the precipitated gel at 100°C for 48 h is beneficial for fabrication of nanostructured t-ZrO_2 with a specific surface area of 77 m^2/g, which is stable up to 850°C.

Acknowledgment This work was financially supported by the State Committee for Scientific Research (KBN) within the project No. 3 T09 147 26.

References

1. Afanasief P, Thiollier A, Breysse M, Dubois JL (1999) Control of the textural properties of zirconium dioxide. Top Catal 8:147–160
2. Barrett EP, Joyner LG, Halenda PH (1951) The determination of pore volume and area distributions in porous substances. J Am Chem Soc 73:373–380
3. Brunauer S, Emmett PH, Teller E (1938) Adsorption of gases in multimolecular layers. J Am Chem Soc 60:309–319
4. Chen S-G, Yin Y-S, Wang D-P (2004) Experimental and theoretical investigation between aqueous precursors structure and crystalline phases of zirconia. J Mol Struct 690:181–187
5. Chraska T, King AH, Berndt ChC (2000) On the size-dependent phase transformation in nanoparticulate zirconia. Mater Sci Eng A 286:169–178
6. Christensen A, Carter EA (1998) First-principles study of the surfaces of zirconia. Phys Rev B 58:8050–8064
7. Chuah GK, Liu SH, Jaenicke S, Li J (2000) High surface area zirconia by digestion of zirconium propoxide at different pH. Microporous Mesoporous Mater 39:381–392
8. Clearfield A (1964) Structural aspects of zirconium chemistry. Rev Pure Appl Chem 14:91–108
9. Clearfiled A, Serrette GPD, Khazi-Syed AH (1994) Nature of hydrous zirconia and sulfated hydrous zirconia. Catal Today 20:195–312
10. Clearfield A, Vaughan PA (1956) The crystal structure of zirconyl chloride octahydrate and zirconyl bromide octahydrate. Acta Crystallogr 9:555–558
11. Dell'Agli G, Ferone C, Mascolo G, Pansini M (2000) Crystallization of monoclinic zirconia from metastable phases. Solid State Ionics 127:223–230
12. Dyrek K, Adamski A, Sojka Z (2001) ZrO_2 as catalyst and catalysts support. In: Yoo H-I, Kang S-JL (eds) Ceramic interfaces 2, IOM communications. Cambridge University Press, London, pp 241–259
13. Garvie RC (1965) The occurrence of metastable tetragonal zirconia as a crystal size effect. J Phys Chem 69:1238–1243
14. Garvie RC, Hannink RH, Pascoe RT (1975) Ceramic steel. Nature 258:703–704
15. Hirata T, Asari E, Kitajima M (1994) Infrared and Raman spectroscopic studies of ZrO_2 polymorphs doped with Y_2O_3 and CeO_2. J Solid State Chem 110:201–207
16. Horvath G, Kawazoe K (1983) Method for the calculation of the effective pore size distribution in molecular sieve carbon. J Chem Eng Jpn 16:470–475
17. Jakubus P, Adamski A, Kurzawa M, Sojka Z (2003) Texture of zirconia obtained by forced hydrolysis of $ZrOCl_2$ solutions. J Therm Anal Calorim 72:299–310
18. Jolivet JP (2000) Metal oxide chemistry and synthesis. Wiley, Chichester
19. Jung KT, Bell AT (2000) The effects of synthesis and pretreatment conditions on the bulk structure and surface properties of zirconia. J Mol Catal A 163:27–42
20. Matsui K, Ohgai M (1997) Formation of hydrous zirconia particles produced by hydrolysis of $ZrOCl_2$ solutions. J Am Ceram Soc 80:1949–1956
21. Matsui K, Ohgai M (2000) Formation mechanism of hydrous-zirconia particles produced by hydrolysis of $ZrOCl_2$ solutions. J Am Ceram Soc 83:1386–1392
22. Mercera PDL, van Ommen JG, Doesburg EBM, Burggraaf AJ, Ross JRH (1991) Zirconia as a support for catalysts. Appl Catal 71:363–391
23. Norman CJ, Goulding PA, McAlpine I (1994) Role of anions in the surface stabilization of zirconia. Catal Today 20:313–322
24. Sánchez-Escribano V, Fernández-López E, Panizza M, Resini C, Gallardo-Amores J-M, Busca G (2003) Characterization of cubic ceria-zirconia powders by X-ray diffraction and vibrational and electronic spectroscopy. Solid State Sci 5:1369–1376
25. Tani E, Yoshimura M, Sōmyia S (1983) Formation of ultrafine tetragonal ZrO_2 powder under hydrothermal conditions. J Am Ceram Soc 66:11–14
26. Wang JA, Valenzuela MA, Salmones J, Vázquez A, García-Ruiz A, Bokhimi X (2001) Comparative study of nanocrystalline zirconia prepared by precipitation and sol-gel method. Catal Today 68:21–30
27. Wells AF (1993) Structural inorganic chemistry. WNiT, Warsaw (Polish edition)
28. Yamaguchi T (1994) Application of ZrO_2 as a catalyst and a catalyst support. Catal Today 20:199–218
29. Zhu WZ, Lei TC, Zhou Y, Ding ZS (1996) Kinetics of isothermal transition from tetragonal to monoclinic phase in ZrO_2 (2 mol% Y_2O_3) ceramic. Mater Chem Phys 44:67–73